Agricultural and Forest Meteorology 322 (2022) 108996

Contents lists available at ScienceDirect

Agricultural and Forest Meteorology

journal homepage: www.elsevier.com/locate/agrformet

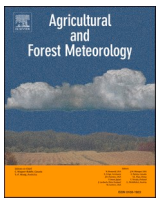

Drought-induced decoupling between carbon uptake and tree growth impacts forest carbon turnover time

Steven A. Kannenberg [a,*], Antoine Cabon [a], Flurin Babst [b,c], Soumaya Belmecheri [c], Nicolas Delpierre [d,e], Rossella Guerrieri [f], Justin T. Maxwell [g], Frederick C. Meinzer [h], David J.P. Moore [b], Christoforos Pappas [i,j,k], Masahito Ueyama [l], Danielle E.M. Ulrich [m], Steven L. Voelker [n], David R. Woodruff [h], William R.L. Anderegg [a]

[a] School of Biological Sciences, University of Utah, Salt Lake City, UT, USA
[b] School of Natural Resources and the Environment, University of Arizona, Tucson, AZ, USA
[c] Laboratory of Tree-Ring Research, University of Arizona, Tucson, AZ, USA
[d] Université Paris-Saclay, CNRS, AgroParisTech, Ecologie Systématique et Evolution, 91405, Orsay, France
[e] Institut Universitaire de France (IUF), France
[f] Department of Agricultural and Food Sciences, University of Bologna, Bologna, Italy
[g] Department of Geography, Indiana University, Bloomington, IN, USA
[h] USDA Forest Service, Pacific Northwest Research Station, Corvallis, OR, USA
[i] Centre d'étude de la forêt, Université du Québec à Montréal, Montreal, QC, Canada
[j] Département Science et Technologie, Téluq, Université du Québec, Montreal, QC, Canada
[k] Department of Civil Engineering, University of Patras, Rio Patras, Greece
[l] Graduate School of Life and Environmental Sciences, Osaka Prefecture University, Sakai, Japan
[m] Department of Ecology, Montana State University, Bozeman, MT, USA
[n] SUNY College of Environmental Science and Forestry, Syracuse, NY, USA

ARTICLE INFO

Keywords:
GPP
Legacy effect
Resilience
Resistance
Tree rings

ABSTRACT

The ability of forests to withstand, and recover from, acute drought stress is a critical uncertainty regarding the impacts of climate change on the terrestrial carbon (C) cycle, but it is unclear how drought responses scale from individual trees to whole forests. Here, we assembled a dataset of tree-ring chronologies co-located within the footprint of eddy covariance towers across North America and Europe, with the aim of quantifying the sensitivity of tree radial growth versus gross primary productivity (GPP) during and following drought. We found that drought induced a large decoupling across C cycle processes, whereby GPP was relatively resistant to water stress despite large reductions in tree-ring widths. This decoupling also occurred in the year following drought (i.e., a 'drought legacy effect'), and was similar in magnitude in response to both summer and winter droughts. By modeling whole-forest C turnover time, we show that a radial growth-GPP decoupling has important ramifications for the forest C cycle, especially if the C not used to support radial growth is instead allocated towards pools with short residence times. Our results demonstrate that quantifications of drought impacts that rely solely on C uptake are missing this fundamental pathway through which drought alters the forest C cycle and the resulting feedbacks to the climate system.

1. Introduction

Forests store nearly half of the carbon (C) in terrestrial ecosystems and take up ~25% of all anthropogenic C emissions (Bonan, 2008; Pan et al., 2011). However, the capacity of forests to assimilate and store C is threatened by an increase in the frequency and severity of droughts (Cook et al., 2015; Dai, 2013; McDowell et al., 2020). The drought resistance (ability to maintain function) and resilience (ability to recover function) of these processes in future climates is a major uncertainty in the terrestrial C cycle (Sippel et al., 2018) yet exerts a significant influence on the climate change mitigation potential of forests worldwide (Anderegg et al., 2020).

* Corresponding author.
E-mail address: s.kannenberg@utah.edu (S.A. Kannenberg).

https://doi.org/10.1016/j.agrformet.2022.108996
Received 3 February 2022; Received in revised form 29 April 2022; Accepted 6 May 2022
Available online 16 May 2022

Current efforts to quantify the resistance and resilience of forests to drought stress have largely been undertaken using tree-ring chronologies (Camarero et al., 2018; Lloret et al., 2011; Merlin et al., 2015). These approaches are invaluable towards understanding the climatic, topographic, and biological mechanisms that underpin the responses of tree growth to drought. However, radial tree growth is only one aspect of a complex forest C cycle, and the relationship between growth and whole-ecosystem fluxes of C is indirect. Thus, several studies have quantified the drought resistance and resilience of C uptake using broader-scale metrics of forest C cycling such as gross primary productivity (GPP) derived from flux towers (He et al., 2018; Shen et al., 2016; Yu et al., 2017). Recent evidence suggests that drought may drive a large decoupling between these processes, whereby structural tree growth is much more sensitive to drought than GPP (Delpierre et al., 2016; Kannenberg et al., 2020b, 2019b).

While this decoupling is intuitive at the tissue-level given the higher drought sensitivity of turgor-driven cell expansion than photosynthesis (Hsiao, 1973) and the plasticity of plant C allocation in response to environmental stress (Epron et al., 2012), evidence at the stand- or ecosystem -scale is scarce due to the paucity of co-located measurements of tree growth and GPP (Babst et al., 2021, though see Cabon et al., 2022 and Krejza et al., 2022). Therefore, our knowledge of the degree of coupling between growth and GPP rests largely on either case studies from a single drought (Kannenberg et al., 2019b), or GPP proxies from models or remote sensing products that may not fully capture both the magnitude of drought impacts or any lagged recovery processes (Anderegg et al., 2015; Kolus et al., 2019; Stocker et al., 2019). Given this lack of evidence, it is unsurprising that most large-scale vegetation models represent allocation to woody tissues as a constant percentage of GPP (Fatichi et al., 2019). Additional uncertainties regarding these processes arise due to the high species-specificity of drought responses, which are underlain by variability in key functional traits. Uncovering the traits that underlie tree drought responses, as well as the coupling between GPP and growth, has the potential to lead to an improved predictive understanding of how drought impacts the forest carbon cycle.

Divergent drought impacts on tree growth versus GPP have vast implications for our understanding of the terrestrial C cycle. Large shifts in allocation from tree boles to pools with shorter residence times (Doughty et al., 2015, 2014; Kannenberg et al., 2019b) have consequences for the turnover time of forest C, the magnitude of which is a major uncertainty in current vegetation models (Carvalhais et al., 2014; Friend et al., 2014; Pugh et al., 2020). Quantifying the differential sensitivity of drought resistance and resilience across distinct C cycle processes and scales could provide valuable insights regarding whether drought impacts are likely to be most apparent through decreased C uptake and productivity, and/or through a shortened C turnover time.

Here, we seek to directly test the hypothesis that drought decouples tree radial growth from ecosystem C uptake. To do so, we amassed a dataset of 38 tree ring chronologies (spanning 31 common gymnosperm and angiosperm species) collected at 16 different eddy covariance tower sites (277 total site-years) that have experienced a severe drought. These chronologies represented the majority of the species present within these towers' footprints, enabling direct comparisons between the resistance and resilience of tree growth and stand-scale GPP. We then explored the implications of a decoupling between growth and GPP for the forest C cycle using a 'box model' that includes fluxes in and out of the main pools of tree structural C. We ask:

1) Are drought resistance and resilience decoupled across C cycle processes?
2) What traits shape variability in resistance and resilience, and what controls the degree of decoupling of these indices across scales?
3) What are the implications of a decoupling between tree radial growth and GPP for whole-forest C turnover?

2. Materials and methods

2.1. Sites and eddy covariance data

We compiled a dataset of 38 tree-ring chronologies collected near or within the footprint of 16 different eddy covariance towers (Fig. 1, Table S1). These sites, located across North America and Europe, spanned a wide variety of ecosystem types and were largely representative of various temperate and arid woodland biomes (Fig. 1), yet all experienced a severe summer or winter drought within the flux record (see below for drought definition). All sites are included in either the FLUXNET2015 Tier 1 (Pastorello et al., 2020, fluxnet.org/data/fluxnet2015-dataset) or AmeriFlux (ameriflux.lbl.gov, downloaded January 6, 2021) datasets.

For the 10 sites in the AmeriFlux network (representing 30 chronologies), net ecosystem exchange data (NEE) was gapfilled using the 50th percentile Ustar distribution and then partitioned into GPP using the nighttime method (Reichstein et al., 2005) as implemented in the R package *REddyProc* (Wutzler et al., 2018). Data that were gapfilled by site PIs were preferentially used, if available. If the NEE variable was not available, turbulent CO_2 flux (FC) was used instead. The meteorological data used for partitioning were taken from the primary sensor (the _1_1_1 suffix). During some periods, there were not enough incoming shortwave radiation data to properly gapfill NEE. In these cases, incoming photosynthetically active radiation (if available) was converted to shortwave, under the assumption that half of the incoming solar irradiance is photosynthetically active radiation (Britton and Dodd, 1976). Data from US-UMB from AmeriFlux are aggregated into both 30-minute (years 2007 – 2019) and 60-minute (years 2000 – 2014) increments. For this site, we used the full 30-minute record for 2007 – 2019 and the 60-minute record for 2000 – 2006. For FLUXNET sites, we used the nighttime partitioned, variable 50th percentile distribution Ustar GPP product (i.e., GPP_NT_VUT_REF), which is the data product most comparable to our AmeriFlux partitioning approach. We confirmed that our partitioning approach was comparable to the FLUXNET2015 data by comparing a subset of 6 sites that were included in both datasets (and thus partitioned independently). At these sites, monthly sums of our GPP product closely matched FLUXNET2015 ($r^2 = 0.98$, slope not significantly different from one).

Some gaps remained even after gapfilling due to sensor malfunction, maintenance, or other long-term gaps. Years with large gaps in GPP during the growing season were excluded from analysis, and the site-years that remained all had $< 5\%$ of GPP records missing.

In order to make GPP (typically aggregated at 30- or 60-minute resolutions) comparable to detrended tree-ring widths (annual resolution, see below for tree-ring detrending methods), we normalized the GPP time series by summing GPP for each site-year and calculating the anomaly for each annual GPP sum (i.e., the percentage deviation from mean GPP at that site). At 11 sites, annual GPP increased or decreased over time, which would bias our calculations of drought responses depending on the year in which the drought occurred. For sites that had a statistically significant (via linear regression, $P < 0.05$) increase or decrease in annual GPP over time, we detrended the GPP time series by taking the residuals of the linear model and normalizing them as above. This quantification of normalized and detrended annual GPP was used for all subsequent analysis.

2.2. Tree ring data

Canopy dominant or co-dominant trees of the common species at each flux site have been previously cored, processed, measured, and crossdated using standard dendrochronological procedures (Speer, 2012; Stokes and Smiley, 1999). Crossdated ring width measurements were detrended using a spline with a 50% frequency cutoff set at two-thirds of the mean sample length (Klesse, 2021), and species-level chronologies (ring width indices, RWI) were built using a bi-weight

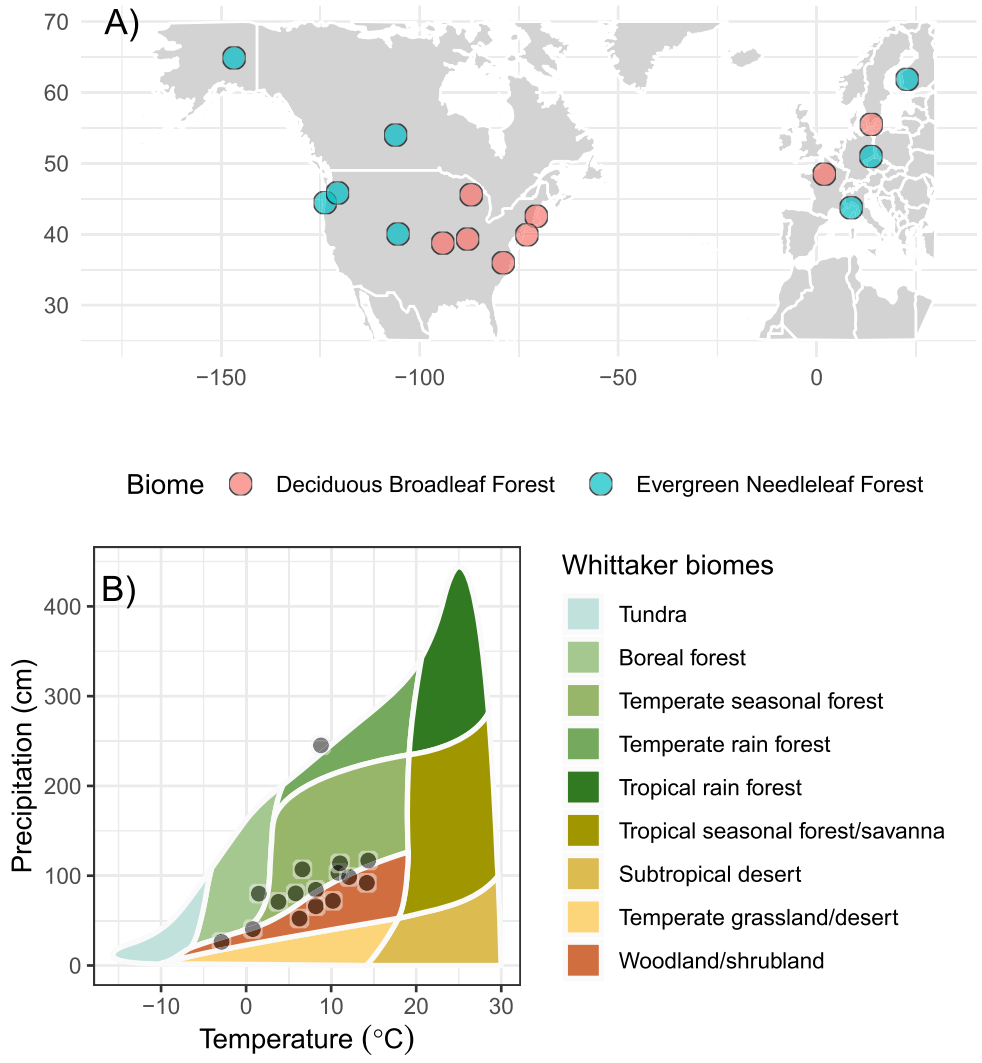

Fig. 1. Map of all eddy covariance towers where tree-ring chronologies were collected (panel A), along with the climate space and biome that our sites represented (panel B).

robust mean-value approach in the R package *dplR* (Bunn, 2008). The distance of each cored tree to the flux tower varied, but all cores were sampled within 1 km of the tower. At least 5 trees were cored for each species at each site, though the average number of cores per site was 55 ± 8.0 (mean ± standard error). Chronology lengths ranged from 30 to 300 years, and the average chronology length was 112.9 years ± 9.8 (mean ± standard error). The average expressed population signal (EPS, which quantifies the signal-to-noise ratio of the time series) for our chronologies was 0.87 ± 0.01 (mean ± standard error). Our results were robust to removing chronologies with an EPS lower than the commonly-used threshold of 0.85 (Fig. S1). However, given that this threshold is arbitrary (Buras, 2017) and a low EPS may simply be indicative of less synchronous tree growth within a stand (a dynamic worth capturing in our study), we elected to not remove chronologies with low EPS for subsequent analyses. Chronology information and statistics are available in Table S2.

We also compiled species composition estimates for all cored tree species at each site (Table S3). These estimates were obtained from the published literature where possible. If published data were not found, species composition estimates were taken from site webpages or obtained directly from site research teams. We used plot-based basal area measurements where possible, but needed to use biomass or canopy cover estimates at a small subset of sites. Citations and data sources for these estimates are available in Table S3. When multiple tree species were present at a flux tower site, we calculated a community-weighted mean RWI using these data, in order to increase comparability to whole-ecosystem measurements of GPP.

2.3. Forest and plant trait data

Site information of location, elevation, mean annual temperature, mean annual precipitation, and IGBP biome were taken from the respective site pages on the AmeriFlux or FLUXNET2015 websites. Functional traits were collected from a variety of different datasets for each of our sampled tree species, including: wood density from the Global Wood Density Database (Chave et al., 2009), specific leaf area and maximum photosynthetic rate from Maire et al. (2015), and hydraulic traits (P50, the water potential at which 50% of xylem conduits are embolized, and the P50 safety margin, which is the difference between P50 and the minimum water potential observed) from the Xylem Functional Traits database (Gleason et al., 2016). Trait data for the analyzed species are available in Table S4.

Drought responses in GPP likely reflect the integrated signal of all constituent species in the tower footprint. Therefore, we aggregated plant trait data to the stand scale in a number of ways: the mean trait value of all cored species, the standard deviation of all cored species, and

the mean of all cored species weighted by species composition.

2.4. Climate data

Standardized Precipitation Evaporation Index v2.6 (SPEI) data for all site-years were used to quantify drought severity (Vicente-Serrano et al., 2010). SPEI data were extracted for two relevant time scales in order to capture the differential effects of growing season versus winter droughts: June – August (hereafter, "Summer") and the previous October – March (hereafter, "Winter").

We calculated mean site climatic water deficit (CWD) as potential evapotranspiration (PET) minus actual evapotranspiration (AET), using data from the TerraClimate dataset (Abatzoglou et al., 2018). Monthly values CWD were extracted for all sites, and these values were summed to get annual CWD. Mean site CWD was calculated over the period 2000 – 2019 in order to reflect climatic conditions during the years when most of our flux tower data were present.

2.5. MODIS data

MODIS leaf area index (LAI) over 8-days windows (MCD15A2H, 500 m pixel size) were obtained for each site from 2002 – 2019 using the R package *MODISTools* (Tuck et al., 2014). In order to make MODIS data comparable to annual GPP sums in ecosystems that experience large annual variation in LAI (e.g., deciduous forests), we limited LAI data to the growing season in each year using a previously published method (Kannenberg et al., 2020a). We considered the start of the growing season to be the first day at which a smoothed curve of daily GPP sums crossed a threshold of mean winter GPP + 30% of the annual smoothed GPP amplitude, and the end of the growing season to be the last time point when smoothed GPP fell below this threshold. Annual growing season LAI means were used in the calculation of drought indices (detailed below), while growing season LAI was also averaged over the entire time interval (2002 – 2019) to calculate mean site LAI and thus quantify the typical canopy cover at each site.

2.6. Calculation of drought indices

To quantify the responses of RWI, GPP, and LAI to severe drought, we calculated metrics of drought resistance and resilience. First, we identified severe drought years within the eddy covariance record at each site. We defined a severe drought as $\alpha < -1.5$ anomaly in SPEI during two different periods: summer (June – August, the peak growing season) and winter (the previous October – March, the start of the hydrological year to early spring). These two periods were chosen to capture any differential effects of a hotter, acute growing season drought (i.e., summer drought) versus a longer-term anomaly in early season moisture storage (i.e., winter drought). Our results were nearly identical when defining a summer drought as the full growing season (April – September), due to significant overlap between the drought years identified with each method (Fig. S2). Any multi-year droughts (i.e., two sequential winter or summer drought years < -1.5 SPEI) were identified and not considered in our analyses to avoid any bias introduced by a few anomalously severe droughts. Likewise, multi-drought years (i.e., a winter and summer drought in the same year) were not included in the analysis (see Table S1 for the drought site-years that were included in our analyses). The selected threshold of drought severity was chosen to represent a severe drought that impacts forest function, yet also be common enough to have a reasonable sample size in our dataset. The threshold of −1.5 SPEI, which corresponds to a return period of 20 years across all sites in our dataset (range = 10 to 33-year return period), is comparable with other studies that have quantified severe drought resistance and resilience (Anderegg et al., 2015; Kannenberg et al., 2019). Our main results were robust to relaxing our threshold to −1.2 SPEI (roughly a drought every 8 years, Fig. S3). When increasing our threshold to −2 SPEI (a once per century event), our sample size decreased drastically to only 4 drought events across all sites (Fig. S4).

Once these severe drought years were identified, we calculated drought resistance (Rt) and resilience (Rs) for the community-weighted RWI (hereafter referred to as "RWI"), annual normalized GPP, and mean growing season LAI as follows:

$$Rt = X_{Drought} \Big/ \underline{X_{Non-drought}}$$

$$Rs = X_{Drought+1} \Big/ \underline{X_{Non-drought}}$$

Where $X_{Drought}$ represents the process of interest (i.e., RWI, GPP, LAI) during the drought year itself, $X_{Drought+1}$ represents the process of interest in the year following a drought, and $\underline{X_{Non-drought}}$ represents the mean of that process in all non-drought years. Thus, these indices are analogous to effect sizes, where Rt represents the impact of each drought on the process of interest relative to normal conditions, and Rs represents the degree to which that process recovered in the year following the drought. These metrics are a slight modification of those developed by Lloret et al. (2011), intended to remove noise related to variability in the pre-drought year (Kannenberg et al., 2019b). Finally, the degree of decoupling between GPP and RWI (denoted ΔRt or ΔRs) was calculated as Rt or Rs in GPP minus Rt or Rs in RWI.

2.7. C turnover time model

In order to quantify the impact of C reallocation away from stem growth and towards other structural tissues, we modeled the mean turnover time of whole-forest structural C using a simple four-pool vegetation C model under a range of different scenarios, whereby the C not allocated to stem growth during the drought year and following year (i.e., Rt and Rs) was re-allocated entirely to leaf, coarse root, or fine root pools instead. Due to the large uncertainties regarding the residence times and allocation dynamics of reproductive tissues and non-structural pools (e.g., sugars/starches, root exudates, respiratory losses), we elected to constrain our analyses to non-reproductive structural components.

To do so, we compiled data for total biomass C density (aboveground and belowground biomass in Mg C ha^{-1}) for the year 2010 from the 300 m grid cell containing all the flux tower sites using the dataset of Spawn et al. (2020). These biomass estimates are almost entirely reflective of tree cover (as opposed to understory vegetation or seedlings) since the underlying dataset for forest biomass is largely based on observations of saplings and mature trees.

After converting to total biomass C within each grid cell (Mg C), that biomass C was partitioned out to each sampled species using our species composition estimates (Table S3). We then allocated that C to leaf, aboveground woody biomass (AWB), coarse root, and fine root pools for each species using allometry derived from the Biomass And Allometry Database (BAAD, Falster et al. (2015), Table S5). For our species, all entries in BAAD that had measurements of total plant mass were considered after entries associated with greenhouse and growth chamber studies were excluded to avoid biases associated with the allometry of seedlings and saplings. From these data, mean percent of biomass contained in leaves, AWB (boles and branches), coarse roots, and fine roots were calculated. Many of our species were not present in this dataset, and thus data were aggregated to the family level or to the plant functional type level (i.e., deciduous angiosperm, deciduous conifer, or evergreen conifer). In some cases, our allometric estimates across tissues had a sum greater than one (expected since these tissue-specific estimates are many times drawing on different data sources). In those cases, values were scaled to sum to one. In order to account for tissue-specific differences in C content, we then scaled these estimates by the percentage of C contained in each tissue. Percent C (by dry mass) data for each tissue were obtained for all species from the TRY database (Kattge et al., 2020, Table S6), and gaps were filled using family-level and then

functional type-level means as above.

The effect of drought on AWB was estimated by quantifying the reduction in basal area increment (BAI) in each species during the drought year itself and in the year after (i.e., Rt and Rs). BAI chronologies were constructed using the 'inside-out' approach in the R package *dplR* (Bunn, 2008). We used this method because diameter measurements were not available for many of our sites.

Reductions in total aboveground woody C (AWC) were estimated by multiplying total AWC by the reduction in stand basal area (the sum of chronology BAI) C represented by the Rt + Rs tree rings. We then simulated the impacts of a re-allocation of AWC on whole-forest C turnover time by adding that lost AWC entirely to leaf, coarse root, or fine root pools.

Whole-forest C turnover time was calculated as follows. First, tissue-specific C density data were converted into a turnover flux (F_{tissue}, in Mg C yr^{-1}) by dividing the total C in each tissue for each species at each site by the mean lifespan (in years) of that tissue (Table S7). Leaf, fine root, and coarse root lifespan data were directly available from TRY, and AWB life span was considered as the mean plant age. Leaf lifespan data for deciduous species were considered to be one year. Tissue lifespan data were aggregated from TRY for each species, and gaps in tissue lifespan data were filled by family and then functional type means. Then, we weighted each tissue-specific F_{tissue} by that species' allometry in order to derive a whole-tree turnover flux, F_{tree}.

$$F_{tree} = \sum(F_{tissue} \times Frac_{tissue})$$

Where F_{tissue} represents the turnover flux of each structural tissue (leaves, AWB, coarse roots, and fine roots) and $Frac_{tissue}$ represents the proportion of total tree biomass contained in each tissue. F_{tree} was then scaled to the whole forest by weighting the F_{tree} of each species by its fractional of total stand basal area.

$$F_{forest} = \sum(F_{tree} \times Frac_{species})$$

Where $Frac_{species}$ represents the proportion of total species composition for each species at each site. Whole-forest C turnover time, τ (in years), was then calculated as the ratio of whole-forest total C density (C_{forest}) to F_{forest} (Pugh et al., 2020; Sierra et al., 2017).

$$\tau = \frac{C_{forest}}{F_{forest}}$$

Finally, we derived a percent change in τ for each of our tissue allocation scenarios, compared to a scenario where there was no reduction in AWC due to drought (i.e., Rt and Rs were 1). Note that this percentage represents the change in whole-forest τ due entirely to allocation shifts in structural C during the drought year itself and the year after, not changes to τ over longer time scales.

2.8. Statistical analysis

Comparisons between categorical variables were conducted using two-tailed t-tests or via pairwise Tukey's HSD for multiple comparisons. Trait correlations were assessed using ordinary least squares regression. For these regressions, normality and homoscedasticity of residuals were confirmed using quantile-quantile and residual plots and were natural log or square root transformed if necessary. All analyses were conducted in the R 4.0 computing environment (R Core Team 2021).

3. Results

Drought resistance (Rt) and resilience (Rs) in radial tree growth

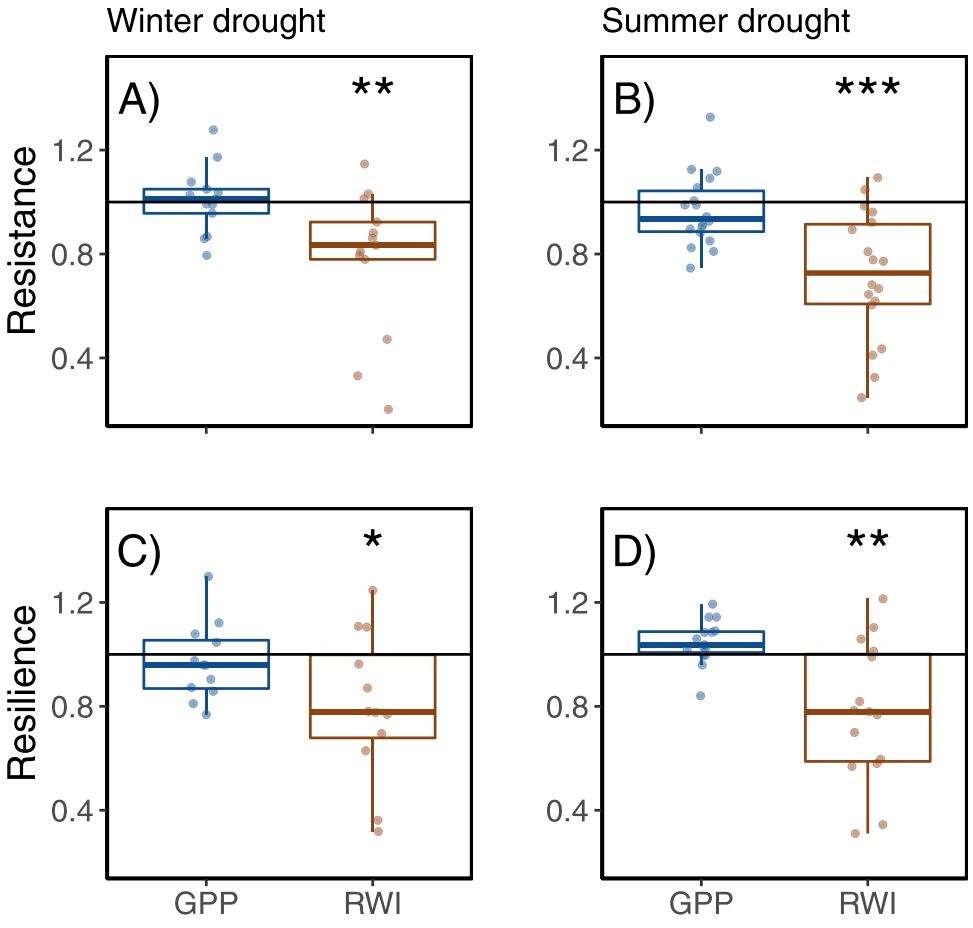

Fig. 2. Resistance (Rt, panels A and B) and resilience (Rs, panels C and D) in normalized gross primary productivity (GPP) and weighted tree-ring width (RWI) in response to two drought periods: winter (October – March, panels A and C) and summer (June – August, panels B and D). The horizontal line represents a value of one, which represents no response to drought. The * symbol indicates a p-value < 0.05 for a *t*-test from one, ** indicates a p-value < 0.01, and *** indicates a p-value < 0.001.

varied widely across species and sites (Fig. S5-S6). Averaged across all drought occurrences, drought reduced community-weighted RWI by 25.4% during the year of the drought itself (i.e., resistance) and by 21.1% in the year after (i.e., resilience, Fig. 2). Lagged drought effects on growth were apparent only one year, with the exception that RWI was significantly reduced for two years following a summer drought (Fig. S7). Rt and Rs were also comparable in response to winter versus summer droughts (Fig. 2). Contrary to the large observed reductions in RWI during and post-drought, annual GPP and growing season LAI remained relatively unchanged, as Rt and Rs were not significantly reduced below one (Fig. 1, Fig. S8-S10).

In general, Rt was correlated with various plant- and site-level traits while Rs was not, though in some cases these relationships differed for summer versus winter droughts (Fig. 3, Fig. S11). Rt calculated from RWI was highest in gymnosperm species and associated with low specific leaf area (SLA) and wood density (WD), though the correlation with WD was not significant following winter droughts. No traits were found to be correlated with Rs calculated from RWI. The traits that predicted Rt and Rs were less consistent for indices derived from GPP. For example, mean P50, mean site precipitation, and mean site water deficit were strong predictors of Rt in response to summer droughts, while there were no significant correlations with Rs. In contrast, Rt in response to winter droughts was best predicted by mean SLA, SLA variability, and P50 variability, while Rs in response to winter droughts was strongly correlated with mean maximum photosynthetic capacity (Amax) and mean LAI.

The degree of decoupling between RWI and GPP Rt during a summer drought was best explained by broad site factors such as elevation ($P < 0.05$, $R^2 = 0.25$) and gymnosperm fraction ($P < 0.05$, $R^2 = 0.20$) instead of plant traits (Fig. 4), though these factors were less successful in explaining the decoupling in Rs. No correlations were found between the degree of RWI-GPP decoupling and any site factors or plant traits following a winter drought.

As a way of estimating the C cycle impacts of the observed decoupling between RWI and GPP, we modeled changes to whole-forest C turnover time (τ) under a range of scenarios, whereby the C not allocated to tree-ring widths was instead allocated to other structural pools. We found ubiquitous decreases in τ across all allocation scenarios (Fig. 5, all $P < 0.01$). Declines in τ were particularly pronounced if C was allocated to leaves (mean change in $\tau = -3.3\%$), due to the large amount of biomass held in foliage and its short lifespan. Decreases in τ were present, but smaller, if C was allocated belowground (-1.2%), due to the small percentage of total biomass held in fine roots (mean = 4.5% of total biomass) and the longer lifespan of coarse roots (mean = 13.75 yrs).

4. Discussion

4.1. Drought decouples GPP and growth

We found that drought induced a striking decoupling between community-weighted tree growth and stand-scale canopy dynamics,

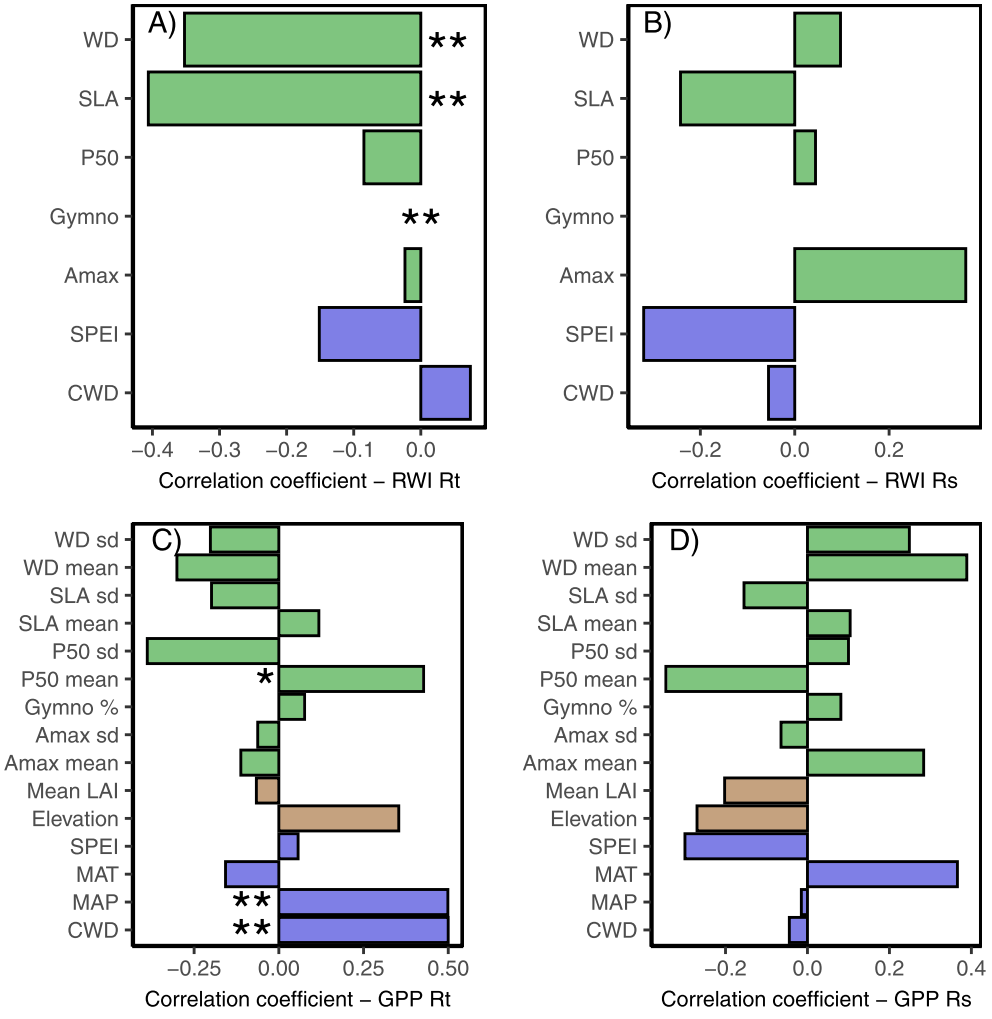

Fig. 3. Pearson's correlation coefficients between Rt (panels A and C) and Rs (panel B and D) in weighted ring width (RWI, panels A and B) and normalized gross primary productivity (GPP, panels C and D) in response to summer droughts for all plant- and site-level traits, including maximum photosynthetic capacity (Amax), mean site climate water deficit (CWD), elevation, taxa (gymnosperm/angiosperm, or% gymnosperm species presence), mean annual temperature/precipitation (MAT/MAP), mean site leaf area index (Mean LAI), the water potential at 50% loss of conductivity (P50), specific leaf area (SLA), SPEI during the drought (SPEI), and wood density (WD). Bar color represents the type of trait: plant (green), climate (blue), or site (brown). The * symbol indicates a p-value < 0.1, while ** indicates a p-value < 0.05. Correlation coefficients are not present for the 'Gymno' trait as these relationships were assessed with t-tests.

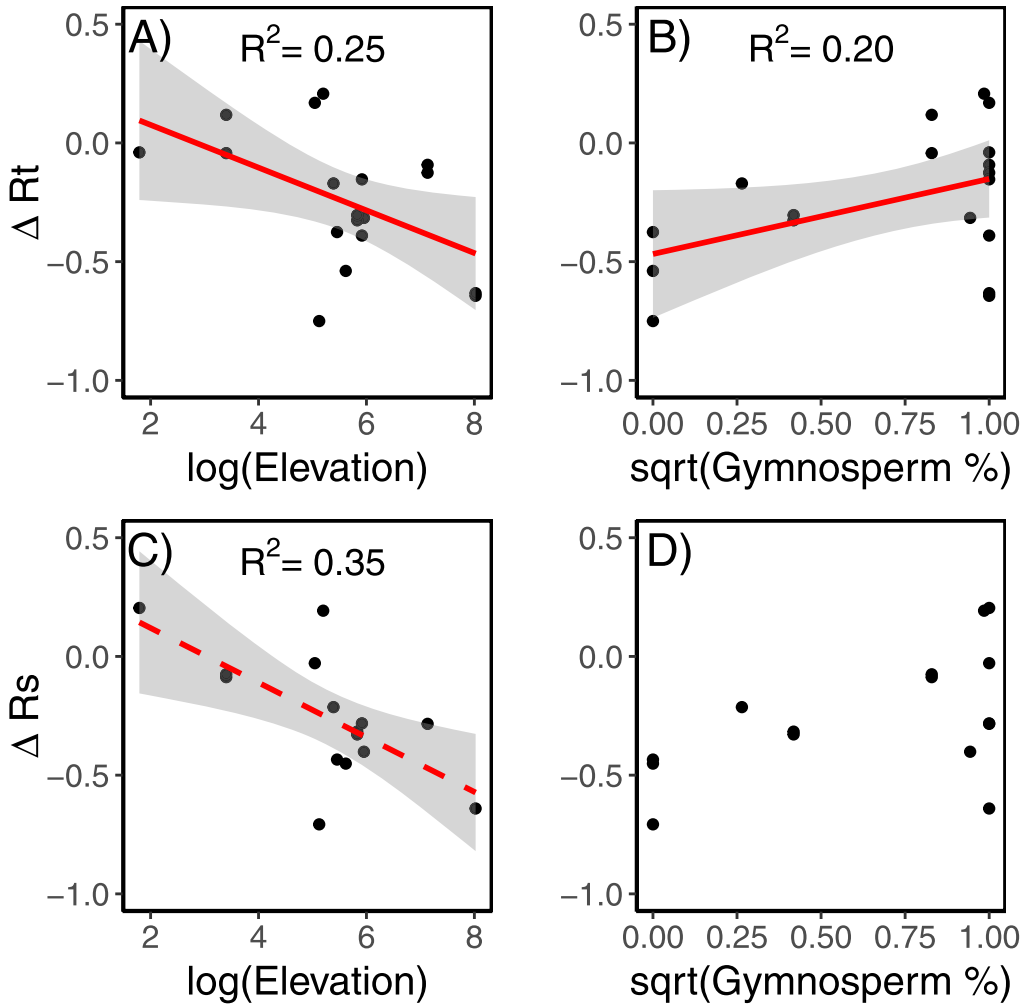

Fig. 4. Relationships between tree-and site-level traits and ΔRt (panels A and B) or ΔRs (panels C and D) in response to summer drought. Solid trendlines are present for significant relationships ($p < 0.05$) and dotted lines represent moderately significant relationships ($p < 0.1$).

whereby RWI was significantly reduced in the year of, and the year after, drought, while total annual GPP and mean LAI were unchanged. While RWI, GPP, and LAI have been known to covary in some cases (Campioli et al., 2016; Teets et al., 2017; Xu et al., 2017), our results add to growing evidence that radial growth and canopy-scale C processes are commonly decoupled (Cabon et al., 2022; Delpierre et al., 2016; Mund et al., 2010; Pappas et al., 2020; Rocha et al., 2006; Seftigen et al., 2018).

We also found the magnitude of Rt and Rs in radial growth to be comparable in response to both summer and winter droughts. Given the strong temperature seasonality at most of our sites, the impacts of winter droughts are likely manifest through reductions in spring water balance and/or an increase in freeze-thaw induced root embolism due to decreased soil insulation from snowpack (Love et al., 2019; Venturas et al., 2017). While many studies on drought responses focus on droughts that occur in the growing season, our results point to the large potential for winter droughts to alter forest C cycling in both arid and mesic forests.

Correlations between drought indices and plant- or site-level traits were generally sparse, though we did find a significant linkage between Rt in radial growth and factors pertaining to investment in tissue longevity such as SLA and WD. Consequently, gymnosperm species had the highest Rt in RWI. There is a robust literature documenting the relationship between investment into leaf longevity and tolerance to environmental stressors, including drought (Wright et al., 2004). Thinner leaves (and leaves in angiosperms generally) are less of a C investment for a tree, and are indicative of a life history strategy more tuned towards fast growth in favorable environmental conditions, whereas higher leaf C investment (as in most gymnosperms) is indicative of more long-lived, stress tolerant species (Greenwood et al., 2017; Grime, 1979). However, contrary to previous work (Anderegg et al., 2015; Vitasse et al., 2019) we found that Rs was not lower for gymnosperm species. High latitude coniferous forests feature more prominently in our dataset than previous studies, and thus this result may indicate a greater ability of gymnosperms in northern or mesic forests to recover from drought stress. The factors underlying the high Rt in GPP were less clear, though we did confirm previous evidence that found embolism resistance (P50), site aridity, and drought severity to mediate the responses of whole-forest C fluxes to drought (Anderegg et al., 2015; Schwalm et al., 2017; Wu et al., 2018), with lower Rt observed in drier forests and in those with lower mean P50.

There is a growing interest in incorporating key plant functional traits to improve the predictive capacity of terrestrial biosphere models (Fatichi et al., 2019; Fisher et al., 2018; Kennedy et al., 2019). However, it stands to reason that different mechanisms control different C cycle processes, and our results confirm that the functional traits underlying drought responses in growth versus C uptake likely differ. Recognizing this nuance is an important factor to consider towards trait-based vegetation modeling.

Multiple mechanisms for the decoupling between RWI and GPP have

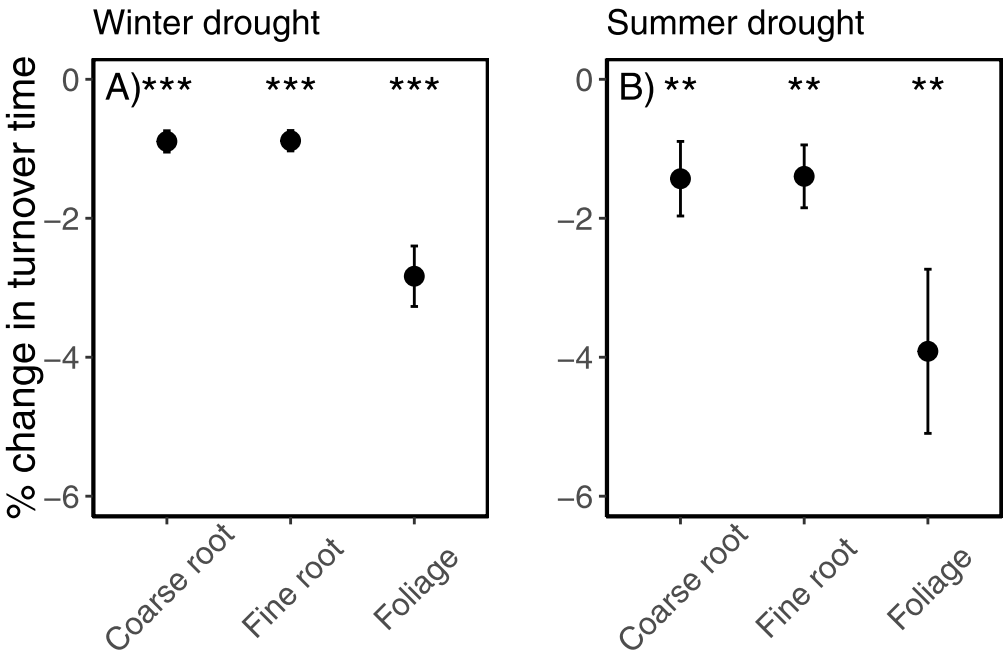

Fig. 5. Change in whole-forest C turnover time in response to winter (panel A) and summer (panel B) droughts based on simulations where the losses of tree ring C during, and following, drought (i.e., Rt and Rs), are allocated entirely to coarse roots, fine roots, or leaves. Dots represent the tissue mean and error bars represent standard error. The * symbol indicates a p-value < 0.05 for a *t*-test from 0, ** indicates a p-value < 0.01, and *** indicates a p-value < 0.001.

been proposed (reviewed in Kannenberg et al., 2020b). A buffering of GPP during drought due to understory species is one such mechanism, though emerging evidence indicates that these species are frequently equally or more drought sensitive than canopy dominant species (Kannenberg et al., 2019b; Rollinson et al., 2021). An abundance of research indicates that a major factor driving this decoupling is likely the weakening of the link between C source activity and radial growth sink dynamics due to: 1) the greater sensitivity of xylogenesis than photosynthesis to aridity, and 2) dynamic C allocation processes (Kannenberg et al., 2019b; Körner, 2015; Mund et al., 2010; Pappas et al., 2020; Peters et al., 2021; Rocha et al., 2006). For example, radial growth is often more sensitive to drought than GPP (Delpierre et al., 2016; Martin-StPaul et al., 2017; Peters et al., 2021), and thus the different sensitivities of these processes could result in radial growth reductions without concomitant declines in GPP. Radial growth is likely also actively reduced during and following drought, whereby C is allocated elsewhere such as non-structural carbon (Körner, 2015), root structural and exudate pools (Phillips et al., 2016), or reproductive efforts (Hacket-Pain et al., 2018).

4.2. Allocation shifts impact turnover time

No matter if the decoupling between RWI and GPP was due to passive or active mechanisms, the C that was fixed yet not used for radial growth necessarily went towards some other structural or non-structural pools. Allocation of C away from long-lived aboveground woody biomass pools could impart profound changes on the forest C cycle irrespective of any drought-induced decline in GPP, because that C is very likely to be allocated towards tissues or compounds with shorter turnover times (Pappas et al., 2020). We estimated that no matter what structural pool C was allocated to, whole-forest C turnover time (τ) was significantly reduced, and this decline was notably large in the foliar allocation scenario. Given that our drought threshold of −1.5 SPEI represented a roughly 20-year drought frequency, our upper-bound estimate of mean τ (where C was allocated to foliar tissue following a summer drought) implies a 0.39% reduction in τ over the lifespan of the forest assuming steady-state vegetation dynamics. The magnitude of this estimate is striking as it is roughly a sixth of the current trend in forest τ (−2.3%) due to increasing tree mortality (Yu et al., 2019). While significant foliar allocation shifts due to drought have been observed at some of our sites (Kannenberg et al., 2019b), widespread canopy allocation across sites seems unlikely given that we did not observe a significant decrease in Rt or Rs derived from MODIS LAI.

These changes in τ are likely a conservative estimate since we only modeled non-reproductive structural C components, which have relatively long residence times. If C were allocated to respiratory fluxes or non-structural compounds, which generally can turn over within days or weeks (Carbone et al., 2007; Muhr et al., 2016), declines in τ would be even more sizeable. Likewise, large-scale allocation to reproductive efforts (e.g., masting events) frequently occurs during or following drought (Hacket-Pain et al., 2018), and is a plausible mechanism for the decoupling between RWI and GPP that would likely reduce τ. Though, the magnitude of this reduction in turnover τ would be highly species-dependent given the high variability in reproductive allocation and tissue residence time across species (Wenk and Falster, 2015). We also note that our model did not include any decomposition dynamics due to uncertainties in decomposition rate over time and across species. Despite these uncertainties, our results provide a first-order approximation of the impacts of drought-induced allocation shifts on the forest C cycle across a range of scenarios. Crucially, our τ modeling reveals that the degree to which the decoupling between RWI and GPP impacts the forest C cycle hinges on where that C is allocated. Further efforts in model development, coupled with increased measurement of allometry and C allocation during and after drought, are necessary steps towards refining our estimates of how this decoupling will impact the ability of forests to mitigate climate change.

5. Conclusions

Drought is likely to cause consequential impacts to the terrestrial C cycle through changes in C uptake, forest structure, and mortality rates (Saatchi et al., 2013; Yang et al., 2018; Yu et al., 2019). Here, we document widespread and direct evidence of an additional, and underappreciated, impact of drought on the forest C cycle: a fundamental disconnect between the responses of tree radial growth versus whole-forest C uptake. We estimate that a drought-induced allocation of

C away from radial growth leads to decreases in whole-forest C turnover time. This evidence indicates that drought impacts on terrestrial C cycling may be significantly mediated by C allocation processes, irrespective of C uptake. Crucially, satellite-based estimates of drought impacts or vegetation models driven by photosynthetic or productivity dynamics may be missing key pathways through which the C cycle will be altered in a changing climate with more frequent and severe drought.

Declaration of Competing Interest

The authors declare that they have no known competing financial interests or personal relationships that could have appeared to influence the work reported in this paper.

Acknowledgements

We thank Ross Alexander and Chad Hanson for contributing tree-ring data, and Seth Spawn for assistance extracting biomass carbon density data. Funding for AmeriFlux data resources were provided by the DOE Office of Science. SAK is supported by the NSF Ecosystem Science cluster grant #1753845, the USDA Forest Service Forest Health Protection Evaluation Monitoring program grant #19–05, and the DOE Environmental System Science program grant #DE-SC0022052. MU is supported by the Arctic Challenge for Sustainability II (JPMXD1420318865). JTM acknowledges support from the US Department of Agriculture National Institute of Food and Agriculture, Agricultural and Food Research Initiative Competitive Program #2017-67013-26191 and Indiana University Vice Provost of Research Faculty.

Supplementary materials

Supplementary material associated with this article can be found, in the online version, at doi:10.1016/j.agrformet.2022.108996.

References

Abatzoglou, J.T., Dobrowski, S.Z., Parks, S.A., Hegewisch, K.C., 2018. TerraClimate, a high-resolution global dataset of monthly climate and climatic water balance from 1958 to 2015. Sci. Data 5, 1–12. https://doi.org/10.1038/sdata.2017.191.

Anderegg, W.R.L., Schwalm, C., Biondi, F., Camarero, J.J., Koch, G., Litvak, M., Ogle, K., Shaw, D., Shevliakova, E., Williams, A.P., Wolf, A., Ziaco, E., Pacala, S., 2015. Pervasive drought legacies in forest ecosystems and their implications for carbon cycle models. Science (80-.) 349, 528–532. https://doi.org/10.1017/CBO9781107415324.004.

Anderegg, W.R.L., Trugman, A.T., Badgley, G., Anderson, C.M., Bartuska, A., Ciais, P., Cullenward, D., Field, C.B., Freeman, J., Goetz, S.J., Hicke, J.A., Huntzinger, D., Jackson, R.B., Nickerson, J., Pacala, S., Randerson, J.T., 2020. Climate-driven risks to the climate mitigation potential of forests. Science (80-.) 368. https://doi.org/10.1126/science.aaz7005.

Babst, F., Friend, A.D., Karamihalaki, M., Wei, J., von Arx, G., Papale, D., Peters, R.L., 2021. Modeling ambitions outpace observations of forest carbon allocation. Trends Plant Sci 26, 210–219. https://doi.org/10.1016/j.tplants.2020.10.002.

Bonan, G.B., 2008. Forests and climate change: forcings, feedbacks, and the climate benefits of forests. Science (80-.) 320, 1444–1449.

Britton, C., Dodd, J., 1976. Relationships of photosynthetically active radiation and shortwave irradiance. Agric. Meteorol. 17, 1–7.

Bunn, A.G., 2008. A dendrochronology program library in R (dplR). Dendrochronologia 26, 115–124. https://doi.org/10.1016/j.dendro.2008.01.002.

Buras, A., 2017. A comment on the expressed population signal. Dendrochronologia 44, 130–132. https://doi.org/10.1016/j.dendro.2017.03.005.

Cabon, A., Kannenberg, S., Arain, A., Babst, F., Baldocchi, D., Belmecheri, S., Delpierre, N., Guerrieri, R., Maxwell, J.T., McKenzie, S., Meinzer, F., Moore, D., Pappas, C., Rocha, A., Szejner, P., Ueyama, M., Ulrich, D., Vincke, C., Voelker, S., Wei, J., Woodruff, D., Anderegg, W., 2022. Cross-biome synthesis of source versus sink limits to tree growth. Science 376, 758–761.

Camarero, J.J., Gazol, A., Sangüesa-Barreda, G., Cantero, A., Sánchez-Salguero, R., Sánchez-Miranda, A., Granda, E., Serra-Maluquer, X., Ibáñez, R., 2018. Forest growth responses to drought at short- and long-term scales in Spain: squeezing the stress memory from tree rings. Front. Ecol. Evol. 6 https://doi.org/10.3389/fevo.2018.00009.

Campioli, M., Malhi, Y., Vicca, S., Luyssaert, S., Papale, D., Peñuelas, J., Reichstein, M., Migliavacca, M., Arain, M.A., Janssens, I.A., 2016. Evaluating the convergence between eddy-covariance and biometric methods for assessing carbon budgets of forests. Nat. Commun. 7, 13717. https://doi.org/10.1038/ncomms13717.

Carbone, M.S., Czimczik, C.I., McDuffee, K.E., Trumbore, S.E., 2007. Allocation and residence time of photosynthetic products in a boreal forest using a low-level 14C pulse-chase labeling technique. Glob. Chang. Biol. 13, 466–477. https://doi.org/10.1111/j.1365-2486.2006.01300.x.

Carvalhais, N., Forkel, M., Khomik, M., Bellarby, J., Jung, M., Migliavacca, M., Mu, M., Saatchi, S., Santoro, M., Thurner, M., Weber, U., Ahrens, B., Beer, C., Cescatti, A., Randerson, J.T., Reichstein, M., 2014. Global covariation of carbon turnover times with climate in terrestrial ecosystems. Nature 514, 213–217. https://doi.org/10.1038/nature13731.

Chave, J., Coomes, D., Jansen, S., Lewis, S.L., Swenson, N.G., Zanne, A.E., 2009. Towards a worldwide wood economics spectrum. Ecol. Lett. 12, 351–366. https://doi.org/10.1111/j.1461-0248.2009.01285.x.

Cook, B.I., Ault, T.R., Smerdon, J.E., 2015. Unprecedented 21st century drought risk in the American Southwest and Central Plains. Sci. Adv. 1 https://doi.org/10.1126/sciadv.1400082.

Dai, A., 2013. Increasing drought under global warming in observations and models. Nat. Clim. Chang. 3, 52–58. https://doi.org/10.1038/nclimate1633.

Delpierre, N., Berveiller, D., Granda, E., Dufrêne, E., 2016. Wood phenology, not carbon input, controls the interannual variability of wood growth in a temperate oak forest. New Phytol. 210, 459–470. https://doi.org/10.1111/nph.13771.

Doughty, C.E., Malhi, Y., Araujo-Murakami, A., Metcalfe, D.B., Silva-Espejo, J., Arroyo, L., Heredia, J.P., Pardo-Toledo, E., Mendizabal, L.M., Rojas-Landivar, V., Vega-Martinez, M., Flores-Valencia, M., Sibler-Rivero, R., Moreno-Vare, L., Viscarra, L., Chuviru-Castro, T., M, O.-.B., Ledezma, R., 2014. Allocation trade-offs dominate the response of tropical forest growth to seasonal and interannual drought. Ecology 95, 2192–2201. https://doi.org/10.1890/13-1507.1.

Doughty, C.E., Metcalfe, D.B., Girardin, C.a.J., Amézquita, F.F., Cabrera, D.G., Huasco, W.H., Silva-Espejo, J.E., Araujo-Murakami, a., da Costa, M.C., Rocha, W., Feldpausch, T.R., Mendoza, a.L.M., da Costa, a.C.L., Meir, P., Phillips, O.L., Malhi, Y., 2015. Drought impact on forest carbon dynamics and fluxes in Amazonia. Nature 519, 78–82. https://doi.org/10.1038/nature14213.

Epron, D., Bahn, M., Derrien, D., Lattanzi, F.A., Pumpanen, J., Gessler, A., Högberg, P., Maillard, P., Dannoura, M., Gérant, D., Buchmann, N., 2012. Pulse-labelling trees to study carbon allocation dynamics: a review of methods, current knowledge and future prospects. Tree Physiol. 32, 776–798. https://doi.org/10.1093/treephys/tps057.

Falster, D.S., Duursma, R.A., Ishihara, M.I., Barneche, D.R., FitzJohn, R.G., Vårhammar, A., Aiba, M., Ando, M., Anten, N., Aspinwall, M.J., Baltzer, J.L., Baraloto, C., Battaglia, M., Battles, J.J., Lamberty, B.B., Van Breugel, M., Camac, J., Claveau, Y., Coll, L., Dannoura, M., Delagrange, S., Domec, J.C., Fatemi, F., Feng, W., Gargaglione, V., Goto, Y., Hagihara, A., Hall, J.S., Hamilton, S., Harja, D., Hiura, T., Holdaway, R., Hutley, L.B., Ichie, T., Jokela, E.J., Kantola, A., Kelly, J.W.G., Kenzo, T., King, D., Kloeppel, B.D., Kohyama, T., Komiyama, A., Laclau, J.P., Lusk, C. H., Maguire, D.A., Le Maire, G., Mäkelä, A., Markesteijn, L., Marshall, J., McCulloh, K., Miyata, I., Mokany, K., Mori, S., Myster, R.W., Nagano, M., Naidu, S.L., Nouvellon, Y., O'Grady, A.P., O'Hara, K.L., Ohtsuka, T., Osada, N., Osunkoya, O.O., Peri, P.L., Petritan, A.M., Poorter, L., Portsmuth, A., Potvin, C., Ransijn, J., Reid, D., Ribeiro, S.C., Roberts, S.D., Rodríguez, R., Acosta, A.S., Santa-Regina, I., Sasa, K., Selaya, N.G., Sillett, S.C., Sterck, F., Takagi, K., Tange, T., Tanouchi, H., Tissue, D., Umehara, T., Utsugi, H., Vadeboncoeur, M.A., Valladares, F., Vanninen, P., Wang, J. R., Wenk, E., Williams, R., De Aquino Ximenes, F., Yamaba, A., Yamada, T., Yamakura, T., Yanai, R.D., York, R.A., 2015. BAAD: a biomass and allometry database for woody plants. Ecology 96, 1445. https://doi.org/10.1890/14-1889.1.

Fatichi, S., Pappas, C., Zscheischler, J., Leuzinger, S., 2019. Modelling carbon sources and sinks in terrestrial vegetation. New Phytol. 221, 652–668. https://doi.org/10.1111/nph.15451.

Fisher, R.A., Christoffersen, O., Longo, M., Viskari, T., Koven, C.D., Anderegg, W.R.L., Dietze, M.C., Farrior, C.E., Holm, J.A., Hurtt, G.C., Knox, R.G., Muller-landau, H.C., Lawrence, P.J., Lichstein, J.W., Shuman, J.K., Verbeeck, H., Powell, T.L., Serbin, S. P., Smith, B., Xu, C., Moorcroft, P.R., 2018. Vegetation demographics in Earth System Models : a review of progress and priorities. Glob. Chang. Biol. 24, 35–54. https://doi.org/10.1111/gcb.13910.

Friend, A.D., Lucht, W., Rademacher, T.T., Keribin, R., Betts, R., Cadule, P., Ciais, P., Clark, D.B., Dankers, R., Falloon, P.D., Ito, A., Kahana, R., Kleidon, A., Lomas, M.R., Nishina, K., Ostberg, S., Pavlick, R., Peylin, P., Schaphoff, S., Vuichard, N., Warszawski, L., Wiltshire, A., Woodward, F.I., 2014. Carbon residence time dominates uncertainty in terrestrial vegetation responses to future climate and atmospheric CO2. Proc. Natl. Acad. Sci. U. S. A. 111, 3280–3285. https://doi.org/10.1073/pnas.1222477110.

Gleason, S.M., Westoby, M., Jansen, S., Choat, B., Hacke, U.G., Pratt, R.B., Bhaskar, R., Brodribb, T.J., Bucci, S.J., Cao, K., Fan, Z., Feild, T.S., Jacobsen, A.L., Johnson, D.M., Domec, J., Mitchell, P.J., Morris, H., Nardini, A., Pittermann, J., Schreiber, S.G., Sperry, J.S., Wright, I.J., Zanne, A.E., 2016. Weak tradeoff between xylem safety and xylem-specific hydraulic efficiency across the worlds woody plant species. New Phytol. 209, 123–136.

Greenwood, S., Ruiz-Benito, P., Martínez-Vilalta, J., Lloret, F., Kitzberger, T., Allen, C.D., Fensham, R., Laughlin, D.C., Kattge, J., Bönisch, G., Kraft, N.J.B., Jump, A.S., 2017. Tree mortality across biomes is promoted by drought intensity, lower wood density and higher specific leaf area. Ecol. Lett. 20, 539–553. https://doi.org/10.1111/ele.12748.

Grime, J., 1979. Plant Strategies and Vegetation Processes. John Wiley & Sons, Ltd., New York, NY.

Hacket-Pain, A.J., Ascoli, D., Vacchiano, G., Biondi, F., Cavin, L., Conedera, M., Drobyshev, I., Liñán, I.D., Friend, A.D., Grabner, M., Hartl, C., Kreyling, J., Lebourgeois, F., Levanič, T., Menzel, A., van der Maaten, E., van der Maaten-Theunissen, M., Muffler, L., Motta, R., Roibu, C.C., Popa, I., Scharnweber, T.,

Weigel, R., Wilmking, M., Zang, C.S., 2018. Climatically controlled reproduction drives interannual growth variability in a temperate tree species. Ecol. Lett. 21, 1833–1844. https://doi.org/10.1111/ele.13158.
He, B., Liu, J., Guo, L., Wu, X., Xie, X., Zhang, Y., Chen, C., Zhong, Z., Chen, Z., 2018. Recovery of ecosystem carbon and energy fluxes from the 2003 Drought in Europe and the 2012 drought in the United States. Geophys. Res. Lett. 45, 4879–4888. https://doi.org/10.1029/2018GL077518.
Hsiao, T.C., 1973. Plant responses to water stress. Annu. Rev. Plant Physiol. 24, 519–570.
Kannenberg, S.A., Bowling, D.R., Anderegg, W.R.L., 2020a. Hot moments in ecosystem fluxes: high GPP anomalies exert outsized influence on the carbon cycle and are differentially driven by moisture availability across biomes. Environ. Res. Lett. 15 https://doi.org/10.1088/1748-9326/ab7b97.
Kannenberg, S.A., Maxwell, J.T., Pederson, N., D'Orangeville, L., Ficklin, D.L., Phillips, R.P., 2019a. Drought legacies are dependent on water table depth, wood anatomy and drought timing across the eastern US. Ecol. Lett. 22, 119–127. https://doi.org/10.1111/ele.13173.
Kannenberg, S.A., Novick, K.A., Alexander, M.R., Maxwell, J.T., Moore, D.J.P., Phillips, R.P., Anderegg, W.R.L., 2019b. Linking drought legacy effects across scales: from leaves to tree rings to ecosystems. Glob. Chang. Biol. 25, 2978–2992. https://doi.org/10.1111/gcb.14710.
Kannenberg, S.A., Schwalm, C.R., Anderegg, W.R.L., 2020b. Ghosts of the past: how drought legacy effects shape forest functioning and carbon cycling. Ecol. Lett. 23, 891–901. https://doi.org/10.1111/ele.13485.
Kattge, J., Bönisch, G., Díaz, S., Lavorel, S., Prentice, I.C., Leadley, P., Tautenhahn, S., Werner, G.D.A., Aakala, T., Abedi, M., Acosta, A.T.R., 2020. TRY plant trait database – enhanced coverage and open access. Glob. Chang. Biol. 26, 119–188. https://doi.org/10.1111/gcb.14904.
Kennedy, D., Swenson, S., Oleson, K.W., Lawrence, D.M., Fisher, R., da Costa, A.C.L., Gentine, P., 2019. Implementing plant hydraulics in the Community Land Model, version 5. J. Adv. Model. Earth Syst. 11, 485–513. https://doi.org/10.1029/2018MS001500.
Klesse, S., 2021. Critical note on the application of the "two-third" spline. Dendrochronologia 65, 125786. https://doi.org/10.1016/j.dendro.2020.125786.
Kolus, H.R., Huntzinger, D.N., Schwalm, C.R., Fisher, J.B., Mckay, N., Fang, Y., Michalak, A.M., Schaefer, K., Wei, Y., Poulter, B., Mao, J., Parazoo, N.C., Shi, X., 2019. Land carbon models underestimate the severity and duration of drought's impact on plant productivity. Sci. Rep. 9, 2758. https://doi.org/10.1038/s41598-019-39373-1.
Körner, C., 2015. Paradigm shift in plant growth control. Curr. Opin. Plant Biol. 25, 107–114. https://doi.org/10.1016/j.pbi.2015.05.003.
Krejza, J., Haeni, M., Darenova, E., Foltýnová, L., Fajstavr, M., Světlík, J., Nezval, O., Bednář, P., Šigut, L., Horáček, P., Zweifel, R., 2022. Disentangling carbon uptake and allocation in the stems of a spruce forest. Environ. Exp. Bot. 196, 104787 https://doi.org/10.1016/j.envexpbot.2022.104787.
Lloret, F., Keeling, E.G., Sala, A., 2011. Components of tree resilience: effects of successive low-growth episodes in old ponderosa pine forests. Oikos 120, 1909–1920. https://doi.org/10.1111/j.1600-0706.2011.19372.x.
Love, D.M., Venturas, M.D., Sperry, J.S., Brooks, P.D., Pettit, J.L., Wang, Y., Anderegg, W.R.L., Tai, X., Mackay, D.S., 2019. Dependence of Aspen stands on a subsurface water subsidy: implications for climate change impacts. Water Resour. Res. 55, 1833–1848. https://doi.org/10.1029/2018WR023468.
Maire, V., Wright, I.J., Prentice, I.C., Batjes, N.H., Bhaskar, R., van Bodegom, P.M., Cornwell, W.K., Ellsworth, D., Niinemets, Ü., Ordonez, A., Reich, P.B., Santiago, L.S., 2015. Global effects of soil and climate on leaf photosynthetic traits and rates. Glob. Ecol. Biogeogr. 24, 706–717. https://doi.org/10.1111/geb.12296.
Martin-StPaul, N., Delzon, S., Cochard, H., 2017. Plant resistance to drought depends on timely stomatal closure. Ecol. Lett. 20, 1437–1447. https://doi.org/10.1111/ele.12851.
McDowell, N.G., Allen, C.D., Anderson-Teixeira, K., Aukema, B.H., Bond-Lamberty, B., Chini, L., Clark, J.S., Dietze, M., Grossiord, C., Hanbury-Brown, A., Hurtt, G.C., Jackson, R.B., Johnson, D.J., Kueppers, L., Lichstein, J.W., Ogle, K., Poulter, B., Pugh, T.A.M., Seidl, R., Turner, M.G., Uriarte, M., Walker, A.P., Xu, C., 2020. Pervasive shifts in forest dynamics in a changing world. Science (80-.) 368. https://doi.org/10.1126/science.aaz9463.
Merlin, M., Perot, T., Perret, S., Korboulewsky, N., Vallet, P., 2015. Effects of stand composition and tree size on resistance and resilience to drought in sessile oak and Scots pine. For. Ecol. Manage. 339, 22–33. https://doi.org/10.1016/j.foreco.2014.11.032.
Muhr, J., Messier, C., Delagrange, S., Trumbore, S., Xu, X., Hartmann, H., 2016. How fresh is maple syrup? Sugar maple trees mobilize carbon stored several years previously during early springtime sap-ascent. New Phytol. 209, 1410–1416.
Mund, M., Kutsch, W.L., Wirth, C., Kahl, T., Knohl, A., Skomarkova, M.V., Schulze, E.D., 2010. The influence of climate and fructification on the inter-annual variability of stem growth and net primary productivity in an old-growth, mixed beech forest. Tree Physiol. 30, 689–704. https://doi.org/10.1093/treephys/tpq027.
Pan, Y., Birdey, R.A., Fang, J., Houghton, R., Kauppi, P.E., Kurz, W.A., Phillips, O.L., Shcidenko, A., Lewis, S.L., Canadell, J.G., Ciais, P., Jackson, R.B., Pacala, S.W., McGuire, A.D., Piao, S., Rautianen, A., Sitch, S., Hayes, D., 2011. A large and persistent carbon sink in the world's forests. Science (80-.) 333, 988–993. https://doi.org/10.1126/science.1201609.
Pappas, C., Maillet, J., Rakowski, S., Baltzer, J.L., Barr, A.G., Black, T.A., Fatichi, S., Laroque, C.P., Matheny, A.M., Roy, A., Sonnentag, O., Zha, T., 2020. Aboveground tree growth is a minor and decoupled fraction of boreal forest carbon input. Agric. For. Meteorol. 290, 108030 https://doi.org/10.1016/j.agrformet.2020.108030.
Pastorello, G., Trotta, C., Canfora, E., Chu, H., 2020. The FLUXNET2015 dataset and the ONEFlux processing pipeline for eddy covariance data. Sci. Data 7, 225. https://doi.org/10.1038/s41597-020-0534-3.
Peters, R.L., Steppe, K., Cuny, H.E., De Pauw, D.J.W., Frank, D.C., Schaub, M., Rathgeber, C.B.K., Cabon, A., Fonti, P., 2021. Turgor – a limiting factor for radial growth in mature conifers along an elevational gradient. New Phytol. 229, 213–229. https://doi.org/10.1111/nph.16872.
Phillips, R.P., Ibáñez, I., D'Orangeville, L., Hanson, P.J., Ryan, M.G., McDowell, N.G., 2016. A belowground perspective on the drought sensitivity of forests: towards improved understanding and simulation. For. Ecol. Manage. 380, 309–320. https://doi.org/10.1016/j.foreco.2016.08.043.
Pugh, T.A.M., Rademacher, T., Shafer, S.L., Steinkamp, J., Barichivich, J., 2020. Understanding the uncertainty in global forest carbon turnover. Biogeosciences 17, 3961–3989.
Reichstein, M., Falge, E., Baldocchi, D., Papale, D., Aubinet, M., Berbigier, P., Bernhofer, C., Buchmann, N., Gilmanov, T., Granier, A., Grunwald, T., Havrankova, K., Ilvesniemi, H., Janous, D., Knohl, A., Laurila, T., Lohila, A., Loustau, D., Matteucci, G., Meyers, T., Miglietta, F., Ourcival, J.M., Pumpanen, J., Rambal, S., Rotenberg, E., Sanz, M., Tenhunen, J., Seufert, G., Vaccari, F., Vesala, T., Yakir, D., Valentini, R., 2005. On the separation of net ecosystem exchange into assimilation and ecosystem respiration: review and improved algorithm. Glob. Chang. Biol. 11, 1424–1439. https://doi.org/10.1111/j.1365-2486.2005.001002.x.
Rocha, A.V., Goulden, M.L., Dunn, A.L., Wofsy, S.C., 2006. On linking interannual tree ring variability with observations of whole-forest CO2 flux. Glob. Chang. Biol. 12, 1378–1389. https://doi.org/10.1111/j.1365-2486.2006.01179.x.
Rollinson, C.R., Alexander, M.R., Dye, A.W., Moore, D.J.P., Pederson, N., Trouet, V., 2021. Climate sensitivity of understory trees differs from overstory trees in temperate mesic forests. Ecology 102, e03264. https://doi.org/10.1002/ecy.3264.
Saatchi, S., Asefi-Najafabady, S., Malhi, Y., Aragão, L.E.O.C., Anderson, L.O., Myneni, R. B., Nemani, R., 2013. Persistent effects of a severe drought on Amazonian forest canopy. Proc. Natl. Acad. Sci. U. S. A. 110, 565–570. https://doi.org/10.1073/pnas.1204651110.
Schwalm, C.R., Anderegg, W.R.L., Michalak, A.M., Fisher, J.B., Biondi, F., Koch, G., Litvak, M., Ogle, K., Shaw, J.D., Wolf, A., Huntzinger, D.N., Schaefer, K., Cook, R., Wei, Y., Fang, Y., Hayes, D., Huang, M., Jain, A., Tian, H., 2017. Global patterns of drought recovery. Nature 548, 202–205. https://doi.org/10.1038/nature23021.
Seftigen, K., Frank, D.C., Björklund, J., Babst, F., Poulter, B., 2018. The climatic drivers of normalized difference vegetation index and tree-ring-based estimates of forest productivity are spatially coherent but temporally decoupled in Northern Hemispheric forests. Glob. Ecol. Biogeogr. 27, 1352–1365. https://doi.org/10.1111/geb.12802.
Shen, W., Jenerette, G.D., Hui, D., Scott, R.L., 2016. Precipitation legacy effects on dryland ecosystem carbon fluxes: direction, magnitude and biogeochemical carryovers. Biogeosciences 13, 425–439. https://doi.org/10.5194/bg-13-425-2016.
Sierra, C.A., Müller, M., Metzler, H., Manzoni, S., Trumbore, S.E., 2017. The muddle of ages, turnover, transit, and residence times in the carbon cycle. Glob. Chang. Biol. 23, 1763–1773. https://doi.org/10.1111/gcb.13556.
Sippel, S., Reichstein, M., Ma, X., Mahecha, M.D., Lange, H., Flach, M., Frank, D., 2018. Drought, heat, and the carbon cycle: a review. Curr. Clim. Chang. Rep. https://doi.org/10.1007/s40641-018-0103-4.
Spawn, S.A., Sullivan, C.C., Lark, T.J., Gibbs, H.K., 2020. Harmonized global maps of above and belowground biomass carbon density in the year 2010. Sci. Data 7, 1–22. https://doi.org/10.1038/s41597-020-0444-4.
Speer, J., 2012. Fundamentals of Tree-Ring Research. The University of Arizona Press, Tucson, AZ. https://doi.org/10.1002/gea.20357.
Stocker, B.D., Zscheischler, J., Keenan, T.F., Prentice, I.C., Seneviratne, S.I., Peñuelas, J., 2019. Drought impacts on terrestrial primary production underestimated by satellite monitoring. Nat. Geosci. 12, 264–270. https://doi.org/10.1038/s41561-019-0318-6.
Stokes, M.A., Smiley, T.L., 1999. An Introduction to Tree-Ring Dating. University of Arizona Press, Tucson, AZ.
Team, R.C., 2021. R: A language and environment for statistical computing.
Teets, A., Fraver, S., Hollinger, D.Y., Weiskittel, A.R., Seymour, R.S., Richardson, A.D., 2017. Linking annual tree growth with eddy-flux measures of net ecosystem productivity across twenty years of observation in a mixed conifer forest. Agric. For. Meteorol. 249, 479–487. https://doi.org/10.1016/j.agrformet.2017.08.007.
Tuck, S.L., Phillips, H.R.P., Hintzen, R.E., Scharlemann, J.P.W., Purvis, A., Hudson, L.N., 2014. MODISTools - downloading and processing MODIS remotely sensed data in R. Ecol. Evol. 4, 4658–4668. https://doi.org/10.1002/ece3.1273.
Venturas, M.D., Sperry, J.S., Hacke, U.G., 2017. Plant xylem hydraulics: what we understand, current research, and future challenges. J. Integr. Plant Biol. 59, 356–389. https://doi.org/10.1111/jipb.12534.
Vicente-Serrano, S.M., Beguería, S., López-Moreno, J.I., 2010. A multiscalar drought index sensitive to global warming: the standardized precipitation evapotranspiration index. J. Clim. 23, 1696–1718. https://doi.org/10.1175/2009JCLI2909.1.
Vitasse, Y., Bottero, A., Cailleret, M., Bigler, C., Fonti, P., Gessler, A., Lévesque, M., Rohner, B., Weber, P., Rigling, A., Wohlgemuth, T., 2019. Contrasting resistance and resilience to extreme drought and late spring frost in five major European tree species. Glob. Chang. Biol. 25, 3781–3792. https://doi.org/10.1111/gcb.14803.
Wenk, E.H., Falster, D.S., 2015. Quantifying and understanding reproductive allocation schedules in plants. Ecol. Evol. 5, 5521–5538. https://doi.org/10.1002/ece3.1802.
Wright, I.J., Reich, P.B., Westoby, M., Ackerly, D.D., Baruch, Z., Bongers, F., Cavender-Bares, J., Chapin, T., Cornelissen, J.H.C., Diemer, M., Flexas, J., Garnier, E., Groom, P.K., Gulias, J., Hikosaka, K., Lamont, B.B., Lee, T., Lee, W., Lusk, C., Midgley, J.J., Navas, M.-L., Niinemets, U., Oleksyn, J., Osada, N., Poorter, H., Poot, P., Prior, L., Pyankov, V.I., Roumet, C., Thomas, S.C., Tjoelker, M.G.,

Veneklaas, E.J., Villar, R., 2004. The worldwide leaf economics spectrum. Nature 428, 821–827. https://doi.org/10.1038/nature02403.

Wu, X., Liu, H., Ciais, P., Flurin, B., Guo, W., Zhang, C., Magliulo, V., Pavelka, M., Liu, S., Huang, Y., Wang, P., Chi, C., Ma, Y., 2018. Differentiating drought legacy effects on vegetation growth over the temperate Northern hemisphere. Glob. Chang. Biol. 24, 504–516. https://doi.org/10.1111/gcb.13920.

Wutzler, T., Lucas-Moffat, A., Migliavacca, M., Knauer, J., Sickel, K., Šigut, L., Menzer, O., Reichstein, M., 2018. Basic and extensible post-processing of eddy covariance flux data with REddyProc. Biogeosciences 15, 5015–5030. https://doi.org/10.5194/bg-15-5015-2018.

Xu, K., Wang, X., Liang, P., An, H., Sun, H., Han, W., Li, Q., 2017. Tree-ring widths are good proxies of annual variation in forest productivity in temperate forests. Sci. Rep. 7 https://doi.org/10.1038/s41598-017-02022-6.

Yang, Y., Saatchi, S.S., Xu, L., Yu, Y., Choi, S., Phillips, N., Kennedy, R., Keller, M., Knyazikhin, Y., Myneni, R.B., 2018. Post-drought decline of the Amazon carbon sink. Nat. Commun. 9 https://doi.org/10.1038/s41467-018-05668-6.

Yu, K., Smith, W.K., Trugman, A.T., Condit, R., Hubbell, S.P., Sardans, J., Peng, C., Zhu, K., Peñuelas, J., Cailleret, M., Levanic, T., Gessler, A., Schaub, M., Ferretti, M., Anderegg, W.R.L., 2019. Pervasive decreases in living vegetation carbon turnover time across forest climate zones. Proc. Natl. Acad. Sci. U. S. A. 116, 24662–24667. https://doi.org/10.1073/pnas.1821387116.

Yu, Z., Wang, J., Liu, S., Rentch, J.S., Sun, P., Lu, C., 2017. Global gross primary productivity and water use efficiency changes under drought stress. Environ. Res. Lett. 12, 014016 https://doi.org/10.1088/1748-9326/aa5258.